nature chemistry

ARTICLES

PUBLISHED ONLINE: 1 MARCH 2009 | DOI: 10.1038/NCHEM.113

Spontaneous assembly and real-time growth of micrometre-scale tubular structures from polyoxometalate-based inorganic solids

Chris Ritchie[1], Geoffrey J. T. Cooper[1], Yu-Fei Song[1], Carsten Streb[1], Huabing Yin[2], Alexis D. C. Parenty[1], Donald A. MacLaren[3] and Leroy Cronin[1]*

We report the spontaneous and rapid growth of micrometre-scale tubes from crystals of a metal oxide-based inorganic solid when they are immersed in an aqueous solution containing a low concentration of an organic cation. A membrane immediately forms around the crystal, and this membrane then forms micrometre-scale tubes that grow with vast aspect ratios at controllable rates along the surface on which the crystal is placed. The tubes are composed of an amorphous mixture of polyoxometalate-based anions and organic cations. It is possible for liquid to flow through the tubes, and for the direction of growth and the overall tube diameter to be controlled. We demonstrate that tube growth is driven by osmotic pressure within the membrane sack around the crystal, which ruptures to release the pressure. These robust, self-growing, micrometre-scale tubes offer opportunities in many areas, including the growth of microfluidic devices and the self-assembly of metal oxide-based semipermeable membranes for diverse applications.

The organization of matter across length-scales[1], starting from well-defined building blocks, is a key challenge in the design of advanced functional materials and devices that can perhaps mimic, or even improve on, nature, using well-defined principles and processes[2]. Many approaches have been proposed for the development of materials that grow from the molecular to the nano- and mesoscale: for example transformation of crystalline materials[3], aggregation of nanoparticles[4], interfacial self-assembly of polymers[5] and amphiphilic systems[6], or combinations of these, to name but a few. Further, the dynamic self-assembly[7] of such systems is very important, because this will help in understanding how matter can be organized under both equilibrium and far-from-equilibrium conditions[8]. As well as possibly providing some important insights regarding the emergence of life[9], understanding such systems may allow the design of functional devices that could take advantage of architectures accessible only under far-from-equilibrium conditions.

Patterned, or highly structured, assemblies can be formed spontaneously in systems that are exposed to fluxes of matter and energy[8]. These assemblies can sustain themselves far from equilibrium while the fluxes are maintained, leading to the emergence of temporal and spatial structures. Key examples are the Belousov–Zhabotinsky (BZ) reaction[10], where an oscillating chemical reaction in a thin film can give rise to temporal pattern formation, and crystal gardens[11–13], in which spatially defined structures are formed by seeding a saturated solution of silicates with a crystal of a transition metal salt. Although these systems are extremely rich, and a vast amount of research has been carried out, they are still poorly understood, and it is very difficult to develop controllable examples in the laboratory to allow systematic studies[13].

In this paper, we report rapid spontaneous microtube emergence (1–120 μm diameter) from a polyoxometalate (POM)-based crystalline solid, **A**, $[(C_4H_{10}NO)_{40}[W_{72}Mn_{12}O_{268}X_7]]_n$ (**A1** when X = Si, **A2** when X = Ge; Fig. 1)[14] in conjunction with a polyaromatic phenanthridinium-based cation (**B** = dihydroimidazophenanthridinium (DIP) or imidazophenanthridinium (IP); Fig. 1)[15,16], by adjustment of the local chemical conditions. Not only are these tubes extremely well defined, they are also highly controllable in terms of diameter, growth rate and even direction of tube growth. The tubes are constructed from a polyoxometalate–organo-cation hybrid, and we have shown that many types of polyoxometalate clusters can be used to form the tubes. This observation is important, because POMs belong to a large family of cluster anions with wide variations in molecular and extended structural motifs constructed from transition metal oxo units linked by shared oxide ions[17]. POMs have much in common with bulk transition metal oxides, and their molecular nature means they have a vast structural diversity[18], with many applications in redox reactions[19], as catalysts[20] and as responsive nanoscale materials[21–24]. POM clusters are extraordinary molecules, as they have a high charge, they are of nanoscale dimensions, and the metal oxide cage can encapsulate many types of small templates and can be formed by self-assembly[25]. Although single crystals of POMs have been observed to undergo transformation to hollow crystal architectures[26], we present here a process that is controllable

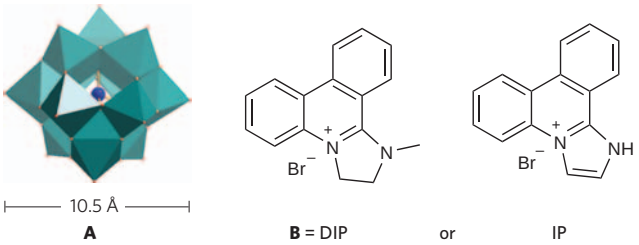

Figure 1 | The molecular building blocks used to form microtubes. Polyoxometalate (POM) **A** is composed of an infinite network of Keggin units (pictured) and reacts with polyaromatic cations **B**: dihydroimidazophenanthridinium (DIP, in this case the *N*-methyl derivative) or imidazophenanthridinium (IP).

[1]WestCHEM, Department of Chemistry, [2]Department of Electronics and Electrical Engineering, [3]Department of Physics and Astronomy, The University of Glasgow, Glasgow G12 8QQ, UK. *e-mail: L.Cronin@chem.gla.ac.uk

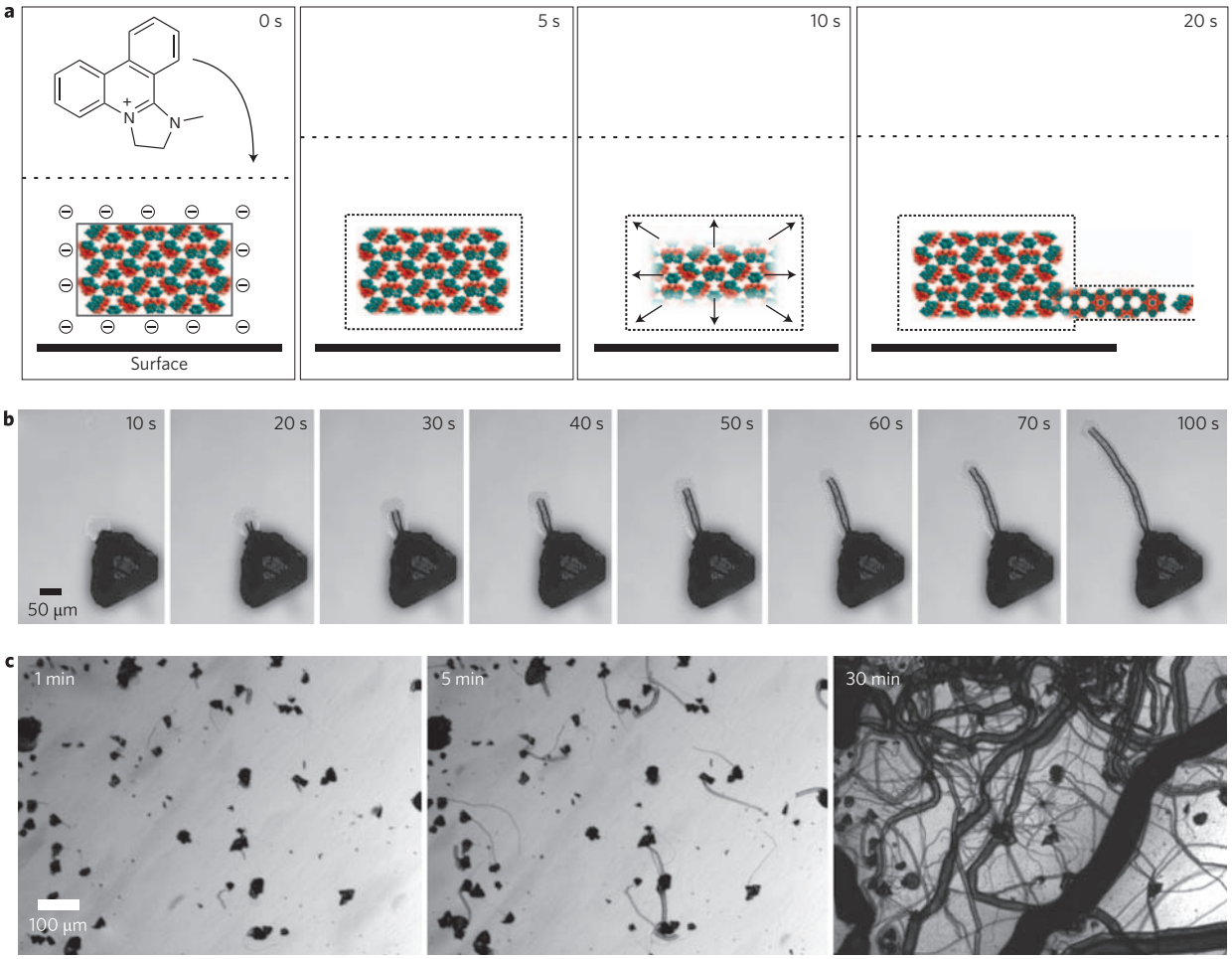

Figure 2 | Spontaneous tube formation from crystals. a, Schematic representation of the initial processes giving rise to the emergence of tubes. Addition of a solution of DIP cations (**B1**) to an anionic crystal of **A** (**A1** or **A2**) results in the formation of a semipermeable membrane around the crystal. The crystal dissolves within the membrane and creates an osmotic pressure. The membrane ruptures, and a tube is formed as dissolved fragments of the crystal come into contact with the solution of **B1. b**, Time-lapse images of a single tube emerging from a crystal. **c**, Images showing a large number of crystals giving rise to many tubes in a bulk system.

and spontaneous, and transforms a range of POM-based materials into tubular architectures and networks in real time.

Results and discussion

A typical set-up for yielding the microtubular structures involves the immersion of a sample of small crystallites (of uniform size distribution) of component **A** into an aqueous solution containing a specific low concentration of component **B** (10–40 mM). The polyoxometalate precursor **A** is only sparingly soluble in aqueous solution, a property that is critical for the formation of the tubular structures. As the outer layers of the crystals begin to dissolve, a semipermeable membrane that is a composite of anionic **A** and cationic **B** molecules is formed around the crystal shell (Fig. 2). Analysis shows that **B** is the only organic constituent of the tube material, and the W:Mn ratio suggests that intact Keggin units from **A** are present. Control of growth rate and diameter is demonstrated by modification of the local chemical environment (concentration of **B**), and directional control is achieved by altering the polarity of an electrode system. The system is sufficiently robust to allow physical manipulation of the growing tube using a micromanipulator, allowing controlled branching, and injection of fluorescent dye shows that the tubes remain hollow and free from fractures that would cause leakage after growth.

The nature of the membrane allows the passage of water, while preventing the entrance of the cation-containing solute or escape of the anionic POM clusters from within the membrane. This behaviour can be likened to a cellular system where the crystal is encapsulated in a hypertonic environment with net flow of water into the membranous sack, and provides the same osmotic driving force that operates in the initial phases of crystal garden formation (indeed, this argument was first used to explain crystal garden growth)[11–13]. Over the course of minutes, the increasing strain on the membrane causes a rupture, resulting in a pressurized jet of POM-enriched solvent being ejected from within the membrane. On contact with the surrounding solution, the polyanionic material is precipitated by the abundant cationic DIP (**B**) in the bulk solvent, forming a cylindrical channel through which the remaining hydrated polyanions then flow. The osmotic pressure in the crystal shell generates a constant flow of dissolved material along the tube, and thereby provides the inorganic material for further tube growth, which occurs predominantly along the surface, until only a hollow shell remains. The sustained growth of the microtubes occurs via a deposition process, whereby combination of the anionic and cationic components at the mouth of the tube results in further assembly of the tube walls while the continuous flow of new material prevents closure (Fig. 2).

The osmotic driving force for the tube growth can be clearly demonstrated by conducting experiments using micromanipulators with femtotips (outer diameter of 1.0 μm) on a growing microtube. If a tube is allowed to grow for some time and is then broken with the manipulator needle, the leading edge of the tube stops growing

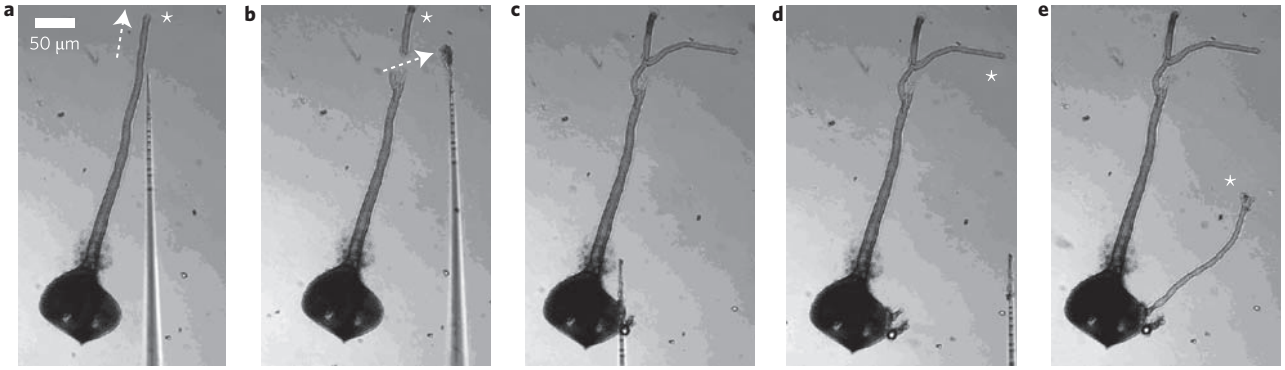

Figure 3 | Micromanipulation is used to control tube growth and branching. a, Normal growth (**A1** and **B1**, direction of growth indicated by the arrow). **b**, The tube has been deliberately broken; the leading edge of the tube (marked with an asterisk *) stops growing and the tube starts re-growing at the breakage point. **c**, A manipulator has been used to rupture the membrane surrounding the crystal, and the tube stops growing. **d**,**e**, The growth of a new tube from the ruptured membrane can be seen (**d**), the continued growth of which is shown in **e**.

immediately and growth is observed to continue from the point of fracture. To provide further support for our proposed growth mechanism, which is essentially an osmotic pump system, we then deliberately ruptured the membranous 'sack/pouch' surrounding the crystal. The tube that had previously been growing from the membrane stopped instantly, and a new tube grew from the site of puncture. This behaviour correlates well with the crystal being surrounded by a single membrane, creating a closed system that exhibits a concerted response to the external stimulus due to pressure release (Fig. 3). Moreover, puncturing the tube deliberately at specific points can be used to design branched tube networks (see Supplementary Fig. S20).

Over the course of the growth process, the tubes may grow to lengths of many millimetres, and as they can typically be grown from many crystals simultaneously on the same surface, collisions occur. Furthermore, the tube growth rate is constant after an initial induction period of up to 60 s, and is independent of tube length. Therefore, after initiation, the tube will grow with an approximately constant diameter as long as there is material left in the crystal. Although the majority of the results here use the POM **A1** or **A2**, we have also conducted preliminary studies showing that almost any POM can be used, subject to the following criteria: (i) low solubility in water and (ii) organic charge-balancing counter-ions (see Supplementary Table S2).

The tube growth process is highly controllable. Once a tube starts growing, its diameter remains constant over the duration of the growth process, and our studies have found that both the rate and the diameter of tube growth can be controlled by the concentration of component **B** added to the solution, for a given surface area of crystal **A**, as shown in Table 1.

As shown in Table 1, the tube diameter can be increased by decreasing the concentration of **B**, and this also decreases the rate of the tube growth process. Using slightly different cation types for **B** (IP) can also give size control between 20 and 130 μm, allowing significantly larger tubes to be constructed (see Supplementary Table S1). Further, by changing the type of precursor **A** (using the Ge template **A2** rather than the Si template **A1**), it is possible to reduce the concentration of organic cation required to grow tubes when using IP, while still retaining the ability to control the overall diameter as shown in Table 1.

When the trajectories of two tubes result in a collision, it has been observed that the two tubes join completely in a merging process, as illustrated in Fig. 4. The exact nature of the merging phenomenon is then dependent on the angle of collision. As seen in Fig. 4a, the head-on collision of two tubes results in merging of the tubes, followed by an almost perpendicular turn in the direction of growth. The merging phenomenon was initially surprising, given the opposing flow directions, with termination perhaps being the more anticipated outcome.

Table 1 | Rate of tube growth under modified conditions.

Components A and B	[B] (mM)	Rate after 1 min ($\mu m\ s^{-1}$)	Rate after 5 min ($\mu m\ s^{-1}$)	Tube diameter (μm)
A1, DIP-Me	38.70	8.3	13.3	20.0
A1, DIP-Me	19.35	2.0	7.3	30.0
A1, DIP-Me	9.67	2.2	2.6	43.3
A1, IP	21.75	12.7	12.7	37.0
A1, IP	5.44	1.8	1.8	130
A2, IP	5.44	4.0	4.0	50.0
A2, IP	1.36	<1	<1	100+

Data showing control over the diameter and rate of growth of microtubes by modifying the type of **A** and the concentration and type of **B**. Crystals of approximately 150 μm (edge length) were used in all cases.

The continued growth after tube fusion demonstrates the substantial pressure that exists within the tubes. Figure 4b shows another variation in the merging process that occurs as a consequence of two individual tubes becoming entangled while growing upwards into the solution. The most informative of the merging phenomena is presented in Fig. 4c, where two tubes of slightly differing diameters grew in contact with one another, and then merged; the process was followed using optical microscopy and a video was generated using screen capture software (see Supplementary Images S6 and S7 and Video S2). This merging process highlights the variation in tube growth rates, which are correlated with tube diameter, and ultimately with the concentration of the solution of **B** (see Table 1). Tubes that initiate at the same time are generally observed to have the same diameter and growth rates; however, tubes that initiate later have a tendency towards larger diameters, owing to the decreased concentration of **B**. This process explains the merging phenomenon shown in Fig. 4c, where the smaller tube growing along the edge of the slightly larger tube is propagating faster, allowing the merging to eventually occur.

Other phenomena that have been observed include helical growth, deflection of the tubes by obstacles, and tube termination (see Supplementary Figs S4–S11). Deflection of tubes during growth typically occurs as a consequence of the height of the obstacle being greater than the tube aperture, with smaller obstacles being overcome by the tubes growing over them. As tubes continue to grow when obstacles are placed in their path, or indeed when their paths are completely blocked, the mechanism for termination is considered to be related to the initiation process. Termination of each tube occurs through narrowing and eventual closing of

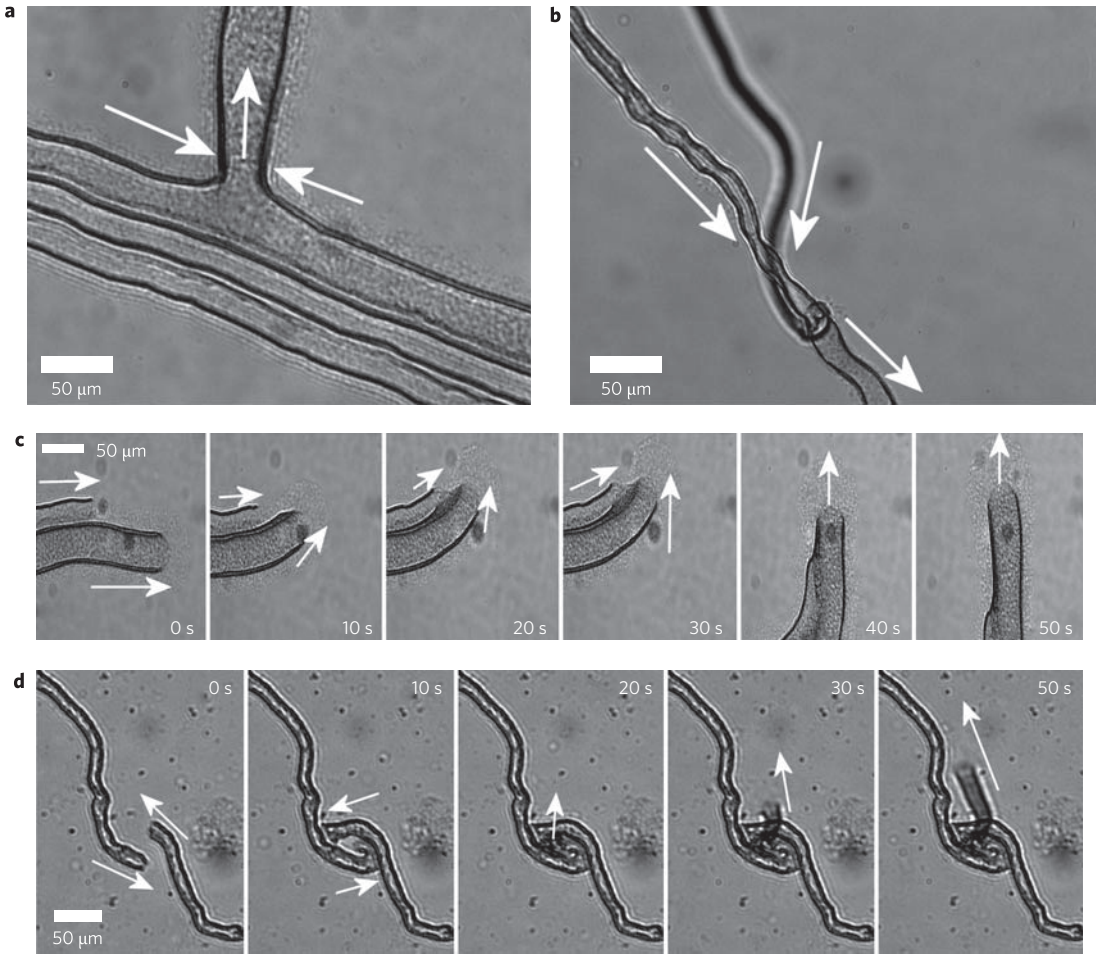

Figure 4 | Different tube-fusion events upon collision. a, Tubes come together and form a new tube at 90° to the trajectory of the joining tubes. **b**, Entangled tubes merge. **c**, Two tubes of different diameter run parallel to one another and then merge. **d**, Collision and entanglement of two tubes, resulting in a merged tube that grows vertically away from the surface.

its aperture, with this process being postulated to occur via equilibration of the system's osmotic pressure, hence halting the flow within the tube. Directional control of the tubes, via deflection, can be achieved either through intervention with a micromanipulator (Fig. 3; see Supplementary Fig. S10 and Video S3) or between polydimethylsiloxane (PDMS) patterns of micro-wells on a glass substrate (see Supplementary Information for details and Fig. S21). Directional control can also be achieved by applying a voltage across the solution soon after tube initiation; by using this technique, the tube can be repeatedly turned through 180° using a bipolar set-up where inverting the polarity of the electrodes induces the directional change (Fig. 5; see Supplementary Video S4). At present, more sophisticated devices are being developed with the aim of having complete directional control over the tube assembly, through the use of multiple-electrode systems and microfluidic devices.

The tubes are also robust enough to receive fluid, injected by a micromanipulator needle, without breaking or leaking. This is shown in Fig. 6, where a fluorescent dye (fluorescein isothiocyanate, 10 mM solution) is injected into the tube and images are recorded in both normal and fluorescence mode.

Both compounds **A** and **B** have a very well-defined molecular structure and have been reported by us before[14–16]. As **A** has the composition $[(C_4H_{10}NO)_{40}[W_{72}Mn_{12}O_{268}X_7]]_n$ (X = Si or Ge), that is, it is a nanoporous network of Keggin ions connected via Mn–O–W bridges with charge-balancing protonated morpholine counter-ions (that is, morpholinium cations) in the pores, it can be postulated that the tubes comprise an ion-exchanged version of the isolated Keggin ions. The bulk elemental composition of tube compound **T1** constructed from **B1** and **A1** was characterized using CHN elemental analysis. To confirm our hypothesis that **B1** is the only organic compound present in the tube walls, the C:N weight ratio of the samples was analysed and compared with the two organic cations present in the reaction system. For **B1**, the C:N weight ratio is 6.83, whereas the morpholinium cation (which originates from **A1**) features a C:N ratio of 3.43. For compound **T1**, a C:N weight ratio of 6.87 was observed, which matches the ratio expected for a purely **B1**-based sample and confirms our initial hypothesis that the only organic counter ion present in compound **T1** is **B1**. Energy-dispersive X-ray (EDX) spectroscopic analysis of the tube walls indicates the presence of tungsten and manganese as the main inorganic building blocks, in an atomic ratio of about 5.5 : 1. This corresponds to the composition of the inorganic precursor **A1**, and suggests that the inorganic Keggin units are retained in the tube walls. However, the only mechanism that is consistent with tube formation is the suggestion that the linked Keggin units in **A1** are dissolved into molecular cluster units, which are subsequently 'pumped' along the tube channels and precipitate as discrete clusters with the organic **B1** cations to form the tube walls. This mechanism is further supported by the complete absence of any crystallographic ordering observed in either high-resolution transmission electron microscopy (TEM) or electron diffraction, which indicates the presence of an amorphous solid and supports our suggested formation mechanism.

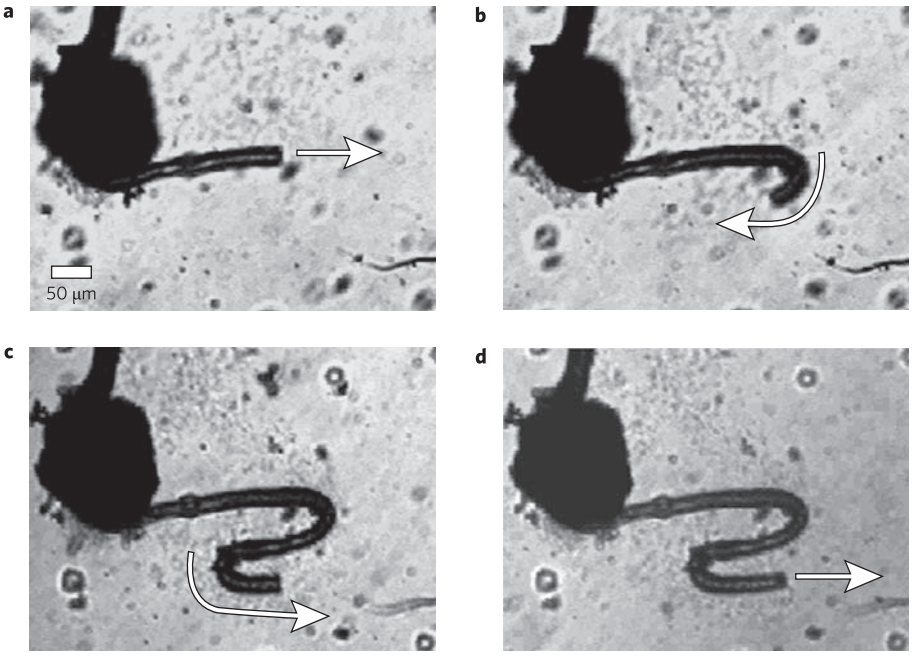

Figure 5 | Control of tube growth direction in a two-electrode system. a–d, A set of still images taken over the course of approximately 3 minutes, showing control of the tube growth direction through application of a voltage across the sample. The electrodes are placed perpendicular to the tube growth shown in **a**, and the crystal lies between them. For a video of this process, see Supplementary Video S4.

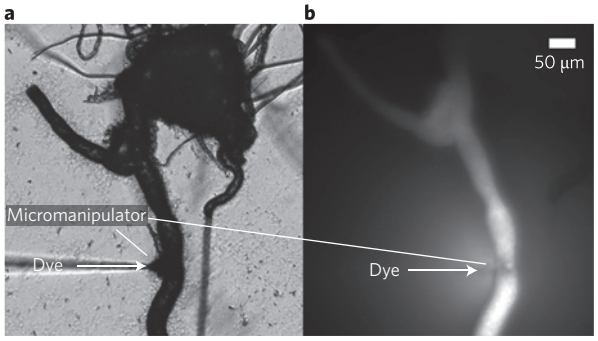

Figure 6 | Injection of fluorescein isothiocyanate dye into a tube. **a**, Normal view, showing the manipulator in the tube. **b**, Fluorescence image, demonstrating that the fluid has travelled into the tube network. For a video of this process, see Supplementary Video S5.

In addition, selected-area EDX (SAEDX) analysis shows that the composition is consistent throughout the length of the tube, which suggests that compound **T1** features the same elemental composition, independent of the spatial position of the SAEDX sample area. See Supplementary Figs S13–S20 for scanning electron microscopy (SEM) and TEM images.

Conclusions

We have presented the first example of spontaneous microtube formation (1–120 μm diameter) from a POM-based crystalline solid $[(C_4H_{10}NO)_{40}[W_{72}Mn_{12}O_{268}X_7]]_n$ (**A1** when X = Si, **A2** when X = Ge) when a very small concentration of a polyaromatic phenanthridinium-based cation (**B** = DIP or IP) is added to the aqueous solution in which the crystal is immersed. Preliminary experiments suggest an initial mechanism similar to that of the processes by which crystal gardens are formed. The tubes tend to grow along the surface of the vessel with controllable diameters and speed, and the direction of growth can be controlled either by modification of the surface properties (physical obstacles or patterned surfaces) or by applying a voltage between two electrodes in solution. Furthermore, the tubes can fuse together to form junctions, and are sufficiently robust to allow solutions to be injected through them without leakage or fracture. Finally, because tube formation does not seem to be limited by POM type, the tubes can be designed to have properties that reflect the building blocks of the parent cluster in terms of redox potential, catalytic activity, charge and photochemical properties. This means that they can be designed to have a variety of functions and applications. Future work will build on these initial results, and will focus on fully understanding the mechanism of tube growth and formation, as well as demonstrating a high level of control, and working towards applications that take advantage of the functionality of the POM material embedded within the walls of the tubes.

Methods

Optical microscopy. Optical microscopy was performed using an Olympus IX81 inverted microscope equipped with a CellR MT20 fluorescence illuminator, Hamamatsu Orca-ER digital camera and two Eppendorf TransferMan micromanipulators. Femtotip needles (1 μm tip) were used for manipulation and injection experiments. Samples were prepared and observed in 1-cm-diameter plastic wells or on standard glass microscope slides.

Electron microscopy. SEM was performed on a Hitachi S-4700 SEM instrument or using a FEI/Philips XL-30 ESEM system with acceleration voltages of 10–20 kV. Samples were prepared by growing the tubes directly on clean silicon wafers. High-resolution TEM and scanning–transmission electron microscopy (STEM) were performed using an FEI Tecnai F20 TEM instrument operating at 200 kV and equipped with a field emission gun and an EDAX EDX spectrometer. Specimens were prepared by dispersing the material in ethanol and then dropping it onto a holey carbon film.

Sample preparation. In a flat-bottomed plastic well (diameter 14 mm), 5 mg (0.22 μmol) of crystalline $(C_4H_{10}NO)_{40}[W_{72}Mn_{12}O_{268}Si_7].48H_2O$ (**A1**) was added to 3 ml of a 20 mM aqueous solution of DIP-Me (**B1**). The reaction mixture was left undisturbed for several minutes, with the progress of the reaction being monitored using an optical microscope (viewing through the bottom of the well). For experiments where micromanipulation was used or when tube material was being collected for analysis, the **A1** crystal was added to a droplet of the **B1** solution on a glass microscope slide or a mica plate. Collection of tube material was achieved by drying the sample after allowing complete consumption of **A1**, followed by several washes with water.

Received 9 October 2008; accepted 22 December 2008; published online 1 March 2009

References

1. Cölfen, H. & Mann, S. Higher-order organization by mesoscale self-assembly and transformation of hybrid nanostructures. *Angew. Chem. Int. Ed.* **42,** 2350–2365 (2003).
2. Mann, S. Life as a nanoscale phenomenon. *Angew. Chem. Int. Ed.* **47,** 5306–5320 (2008).
3. Banfield, J. F., Welch, S. A., Zhang, H., Ebert, T. T. & Penn, R. L. Aggregation-based crystal growth and microstructure development in natural iron oxyhydroxide biomineralization products. *Science* **289,** 751–754 (2000).
4. Liu, T. B., Diemann, E., Li, H. L., Dress, A. W. M. & Müller, A. Self-assembly in aqueous solution of wheel-shaped Mo_{154} oxide clusters into vesicles. *Nature* **426,** 59–62 (2003).
5. Capito, R. M., Azeveo, H. S., Velichko, Y. S., Mata, A. & Stupp, S. L. Self-assembly of large and small molecules into hierarchically ordered sacs and membranes. *Science* **319,** 1812–1816 (2008).
6. Zhang, J., Song, Y. S., Cronin, L. & Liu, T. B. Self-assembly of organic–inorganic hybrid amphiphilic surfactants with large polyoxometalates as polar head groups. *J. Am. Chem. Soc.* **130,** 14408–14409 (2008).
7. Chichak, K. S. *et al.* Molecular Borromean rings. *Science* **304,** 1308–1312 (2004).
8. Maselko, J. & Strizhak, P. Spontaneous formation of cellular chemical system that sustains itself far from thermodynamic equilibrium. *J. Phys. Chem. B* **108,** 4937–4939 (2004).
9. Cairns-Smith, A.-G. Chemistry and the missing era of evolution. *Chem. Eur. J.* **14,** 3830–3839 (2008).
10. Yang, L. F., Dolnik, M., Zhabotinsky, A. M. & Epstein, I. R. Oscillatory clusters in a model of the photosensitive Belousov–Zhabotinsky reaction system with global feedback. *Phys. Rev. E* **62,** 6414–6420 (2000).
11. Collins, C., Zhou, W., Mackay, A. K. & Klinowski, J. The 'silica garden': a hierarchical nanostructure. *Chem. Phys. Lett.* **286,** 88–92 (1998).
12. Cartwright, J. H. E., Garcí-Ruiz, J. M., Novella, M. L., & Otálora, F. Formation of chemical gardens. *J. Colloid Interface Sci.* **256,** 351–359 (2002).
13. Thouvenel-Romans, S. & Steinbock, O. Oscillatory growth of silica tubes in chemical gardens. *J. Am. Chem. Soc.* **125,** 4338–4341 (2003).
14. Ritchie, C. *et al.* Reversible redox reactions in an extended polyoxometalate framework solid. *Angew. Chem. Int. Ed.* **47,** 6881–6884 (2008).
15. Parenty, A. D. C., Smith, L. V., Pickering, A. L., Long, D.-L. & Cronin, L. General one-pot, three-step methodology leading to an extended class of N-heterocyclic cations: spontaneous nucleophilic addition, cyclization, and hydride loss. *J. Org. Chem.* **69,** 5934–5946 (2004).
16. Parenty, A. D. C. *et al.* Discovery of an imidazo-phenanthridine synthon produced in a five-step one-pot reaction leading to a new family of heterocycles with novel physical properties. *Chem. Commun.* 1194–1196 (2006).
17. Long, D.-L., Burkholder, E. & Cronin, L. Polyoxometalate clusters, nanostructures and materials: from self assembly to designer materials and devices. *Chem. Soc. Rev.* **36,** 105–121 (2007).
18. Müller, A., Shah, S. Q. N., Bögge, H. & Schmidtmann, M. Molecular growth from a Mo_{176} to a Mo_{248} cluster. *Nature* **397,** 48–50 (1999).
19. Long, D.-L., Abbas, H., Kögerler, P. & Cronin, L. Confined electron-transfer reactions within a molecular metal oxide 'Trojan Horse'. *Angew. Chem. Int. Ed.* **44,** 3415–3419 (2005).
20. Rhule, J. T., Neiwert, W. A., Hardcastle, K. I., Do, B. T. & Hill, C. L. $Ag_5PV_2Mo_{10}O_{40}$, a heterogeneous catalyst for air-based selective oxidation at ambient temperature. *J. Am. Chem. Soc.* **123,** 12101–12102 (2001).
21. Long, D.-L. & Cronin, L. Towards polyoxometalate-integrated nano systems. *Chem. Eur. J.* **12,** 3698–3706 (2006).
22. Song, Y.-F. *et al.* Design of hydrophobic polyoxometalate hybrid assemblies beyond surfactant encapsulation. *Chem. Eur. J.* **14,** 2349–2354 (2008).
23. Long, D.-L., Streb, C., Song, Y.-F., Mitchell, S. G. & Cronin, L. Unravelling the complexities of polyoxometalates in solution using mass spectrometry: protonation versus heteroatom inclusion. *J. Am. Chem. Soc.* **130,** 1830–1832 (2008).
24. Song, Y.-F. *et al.* From polyoxometalate building blocks to polymers and materials: the silver connection. *J. Mater Chem.* **17,** 1903–1908 (2007).
25. Song, Y.-F., Long, D.-L. & Cronin, L. Non covalently connected frameworks with nanoscale channels assembled from a tethered polyoxometalate–pyrene hybrid. *Angew. Chem. Int. Ed.* **46,** 3900–3904 (2007).
26. Xin, Z. *et al.* Keggin POM microtubes: a coincident product of crystal growth and species transformation. *Inorg. Chem.* **45,** 8856–8858 (2006).

Acknowledgements

The authors would like to thank the Leverhulme Trust (London), the Royal Society, the University of Glasgow, WestCHEM and the EPSRC for funding.

Author contributions

L.C. conceived and designed the experiments, analysed the data, and prepared the manuscript, with help from C.S., C.R. and G.C. C.R. synthesized the clusters and the tubes, A.P. synthesized the cations, G.C., C.R., H.Y. and Y.S. performed the experiments with the tubes, and H.Y. fabricated the patterned structures. C.S. and D.M. performed the electron microscopy.

Additional information

Supplementary information accompanies this paper at www.nature.com/naturechemistry. Reprints and permission information is available online at http://npg.nature.com/reprintsandpermissions/. Correspondence and requests for materials should be addressed to L.C.